

Journal of Marine Science and Technology; Vol. 17, No. 4B; 2017: 161-166  
DOI: 10.15625/1859-3097/17/4B/13004  
<http://www.vjs.ac.vn/index.php/jmst>

## THE APPLICATION OF SPLIT STEP FOURIER MIGRATION TO INTERPRETING GPR DATA IN VIETNAM

Dang Hoai Trung<sup>1\*</sup>, Nguyen Van Giang<sup>2</sup>, Nguyen Thanh Van<sup>1</sup>,  
Nguyen Van Thuan<sup>1</sup>, Vo Minh Triet<sup>1</sup>

<sup>1</sup>University of Science, Vietnam National University-Ho Chi Minh City

<sup>2</sup>Institute of Geophysics, VAST

\*E-mail: dhtrung@hcmus.edu.vn

Received: 9-11-2017

**ABSTRACT:** Migration methods play an essential role in processing ground penetrating radar data. For estimating electromagnetic propagation velocity distribution, the finite - difference migration is used because of its reliable performance with high noise conditions. To optimize this migration algorithm, we propose using energy diagram as a criterion of looking for the correct velocity. If the velocity varies laterally and vertically, split step Fourier migration is used for creating a true image of subsurface structures. We applied these steps to real data in Vietnam. The results verified on field data show that migrated images with calculated velocity from energy diagram have the best quality.

**Keywords:** Split Step Fourier Migration, energy diagram, finite - difference migration.

### INTRODUCTION

Ground Penetrating Radar (GPR) is the most accurate and fast method in surveying near-surface structure. There are four main steps for processing GPR data: Removing bad data, filtering noise, gaining, calculating electromagnetic propagation velocity and migration. In seismic method, migration is usually the last step for collapsing diffraction hyperbolae on unmigrated sections to points, thus moving reflection events to their proper locations, creating a true image of subsurface structures. Nowadays, in GPR, migration becomes the middle step of processing data for estimating true velocity [1, 2].

There are two types of migration methods: Time and depth migration. In time migration, we assumed that the velocity is constant, thus RMS velocity is used. However, the real environment is very sophisticated, the

propagation velocity varies in both lateral and vertical directions. Therefore, the depth migration that uses interval velocity is better than time migration in some cases.

### SPLIT STEP FOURIER MIGRATION

Phase shift is a migration method based on wavefield extrapolation [3]. Phase shift is performed in the frequency wave number domain, so a constant velocity must be used for each depth interval being migrated. To solve this problem, phase shift plus interpolation is introduced. In this method, some constant velocity migrations are implemented for each migration interval and the results are combined to form last migrated section [4].

The SSF migration algorithm is an alternative to above methods. It is based on a modification to phase shift migration that makes it possible to accommodate lateral variations in the velocity for each migration

interval. The lateral changes are considered as a perturbation, and therefore only one additional spatial Fourier transform is required for each depth extrapolation. We can split the laterally varying velocity field into a constant term and a small perturbation term [3]:

$$v_{x,z} = v_0 z + \delta v_{x,z} \quad (1)$$

Firstly, we use  $v_0(z)$  to propagate wavefields in the  $(\omega, k_x)$  domain [3]:

$$P^* = P_{z,k_x,\omega} \exp \left[ \pm i \sqrt{\left( \frac{\omega}{v_0 z} \right)^2 - k_x^2} dz \right] \quad (2)$$

Then,  $P^*$  is transformed back to the  $(\omega, x)$  domain, and a phase correction is applied to it to account for the lateral velocity variation [3]:

$$P_{z+dz,k_x,\omega} = \hat{P}^* \exp \left[ \pm i \left( \frac{\omega}{v_{x,z}} + \frac{\omega}{v_0 z} \right) dz \right] \quad (3)$$

The accuracy of SSF can be improved by making the propagator symmetric, that is, by splitting the phase shift term into two identical parts and applying them before and after the wave propagation in the  $(\omega, k_x)$  domain [3]:

$$\pm i \left( \frac{\omega}{v_{x,z}} - \frac{\omega}{v_0 z} \right) dz = \pm \left( 2 * \frac{1}{2} \right) \left( \frac{\omega}{v_{x,z}} - \frac{\omega}{v_0 z} \right) dz \quad (4)$$

However, for strong lateral variation of the velocity field, the perturbation theory fails, and more than one reference velocity must be used for SSF.

## FIELD DATA

In this part, we illustrate the accuracy of SSF migration with some real data.

### Underground construction in Ho Chi Minh city street

The GPR data were collected by Detector

Duo (IDS - Italy) with 700 MHz shielded antenna on a street of district 3, Ho Chi Minh city. In this GPR section after filtering noise (fig. 1), we can see two hyperbole signals at 2.4 m and 5.4 m of distance. The polarity of the reflection from the top of those two objects is reversed, thus they are high conductive anomalies. According to our prior information, this line crosses two subsurface metal water pipes [5].

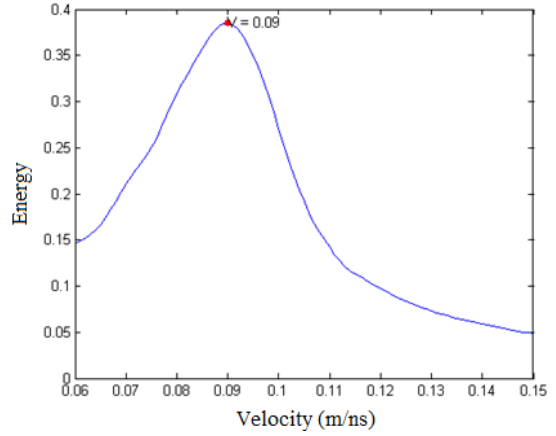


Fig. 1. Energy diagram of zone around the first hyperbole

The GPR section in fig. 2 will be processed by finite-difference migration with the RMS velocity range of 0.06 m/ns to 0.15 m/ns (its jump valued 0.001 m/ns). We estimate a set of the total energy values extracted from migrated results with different velocities for one specific zone. This zone is illustrated as a dashed rectangle in fig. 2. Each total energy value is the summation of all energy points of migrated section from one velocity. Therefore, we can achieve a graph expressing relationship between total energy values and velocities [6]. Note that energy is square of amplitude.

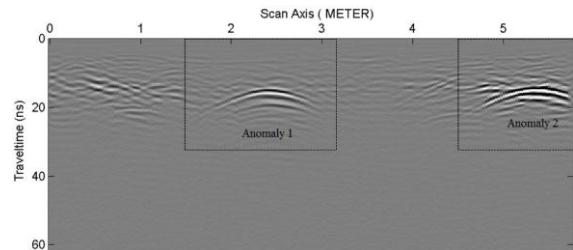


Fig. 2. GPR section after processing

The result shows that the calculating signal zone around the first hyperbole has maximum energy value at the velocity of 0.09 m/ns (fig. 1). Similarly, we also estimate the energy diagram of the second hyperbole. The results in fig. 3 show that the EM wave velocity in the environment above anomaly 2 is equal to 0.093 m/ns.

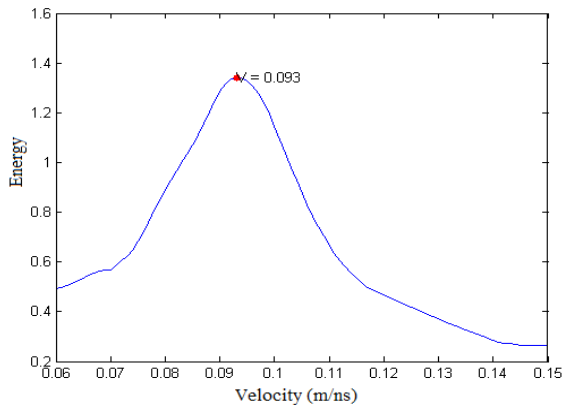


Fig. 3. Energy diagram of zone around the second hyperbole

As such, the use of maximum energy standard in order to optimize the migration problem has shown the lateral variations in velocity in this survey area. Therefore, SSF will be applied to migrate the GPR section (fig. 4). On the migrated section, the two signals are clear and convergent. Consequently, the propagation velocities to the top of two hyperbolae are true. The depths and sizes of the two pipes based on the calculated velocity are  $d_1 = 0.65$  m;  $\Phi_1 = 142$  mm and  $d_2 = 0.68$  m;  $\Phi_2 = 142$  mm respectively. This result has proven the accuracy of research method.

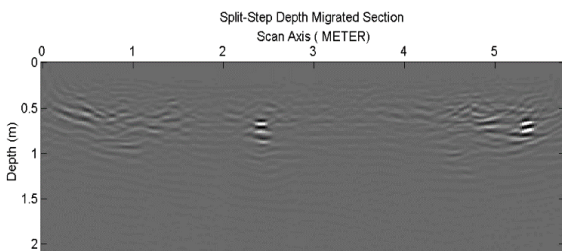


Fig. 4. The GPR migrated section by SSF

### Surveying geology in Khanh Hoa province

The GPR data were collected by Zond 12e (Radar System - Latvia) with 150 MHz unshielded antenna at the seashore of Cam Lam district, Khanh Hoa province. The purpose of this survey is to determine the depth of a shell deposit layer. There are 5 longitudinal lines and 15 transverse lines at this survey area.

Based on data from two electrical resistivity imaging sections and a geological borehole, there are three layers in the survey site:

The first layer has rather low resistivity values which range from 120  $\Omega$ m to 160  $\Omega$ m. This layer can be interpreted as fine sand with its thickness of 3 m. It has been formatted from white grey, white yellow fine sand. It is in wet and loose state.

The second layer has low resistivity values which range from 70  $\Omega$ m to 120  $\Omega$ m. This layer is also fine sand the same as the above layer, but it is in wet and medium dense to dense state.

The last layer resistivity values are lower than 70  $\Omega$ m. This layer is muddy clay which consists of bluish grey, whitey grey, organic muddy clay. It is high plasticity and in water saturated and very soft state.

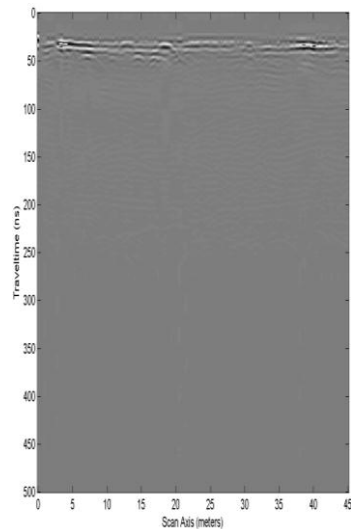


Fig. 5a. The raw GPR section of line 5

We use the transverse lines 5 and 14 to show the essential and accuracy of SSF migration. Fig. 5a is raw section of line 5 and

fig. 5b is the section after processing. We can find a lot of hyperbolae in this image at  $x_1 = 14$  m,  $t_1 = 22$  ns;  $x_2 = 5.2$  m,  $t_2 = 52$  ns;  $x_3 = 20.6$  m,  $t_3 = 126$  ns and  $x_4 = 19.6$  m, 222 ns. Several hyperbolae at the depth of 200 to 250 ns can be reflection signals from the shell deposits. From 250 ns to 450 ns, the signal intensity decreases quickly due to low resistivity environment.

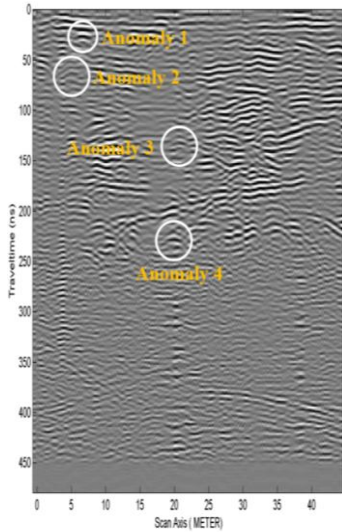


Fig. 5b. The GPR section of line 5 after processing

This GPR section will be processed by finite-difference migration with the RMS velocity range of 0.07 m/ns to 0.16 m/ns (its jump valued 0.001 m/ns) for signal zone around the first anomaly. The energy diagram (fig. 6a) shows that the velocity at the apex of the hyperbola 1 (RMS velocity) is 0.141 m/ns (the highest energy).

Similarly, the RMS velocity at the apex of the anomalies 2, 3 and 4 can be estimated at 0.111, 0.086 and 0.073 m/ns respectively from energy diagrams (figures 6b, 6c, 6d). To build the velocity model of this site, we must have the interval velocities derived from RMS velocities. The relevant formula of interval velocity and RMS velocity is shown as below:

$$v_{int} = \sqrt{\frac{v_{rms2}^2 \tau_2 - v_{rms1}^2 \tau_1}{\tau_2 - \tau_1}} \quad (5)$$

We calculate the interval velocities by using the above equation and build the velocity model of this survey area as shown below (fig. 7) [7]. We can see that the velocity varies strongly in vertical direction due to the change of water content of the coastline.

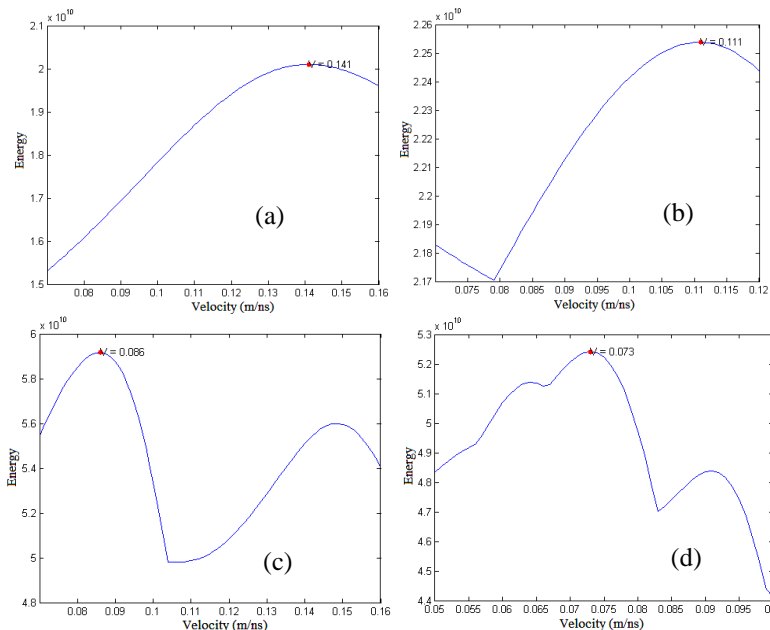


Fig. 6. The energy diagram of signal zone around the anomaly a) 1, b) 2, c) 3, d) 4

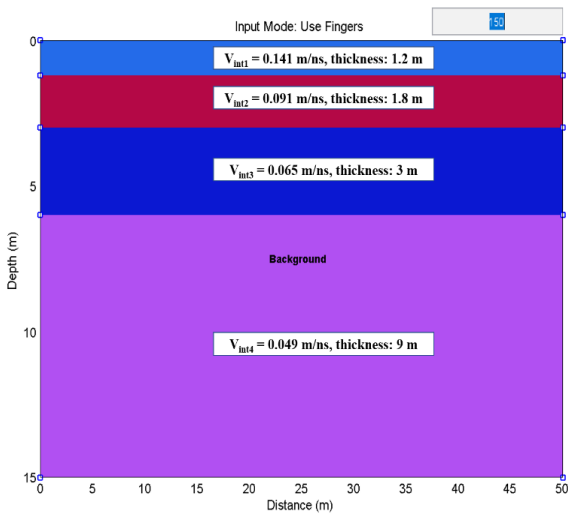


Fig. 7. The velocity model

The SSF migrated section 5 using the above velocity model is shown in fig. 8. Evidently, all hyperbolae are convergent and the geological boundaries are clear and visible. The time axis is changed to depth axis; thus, we can determine the depth of geological boundaries. The shell deposit layer can be recognized at the depth of 6 - 8 m.

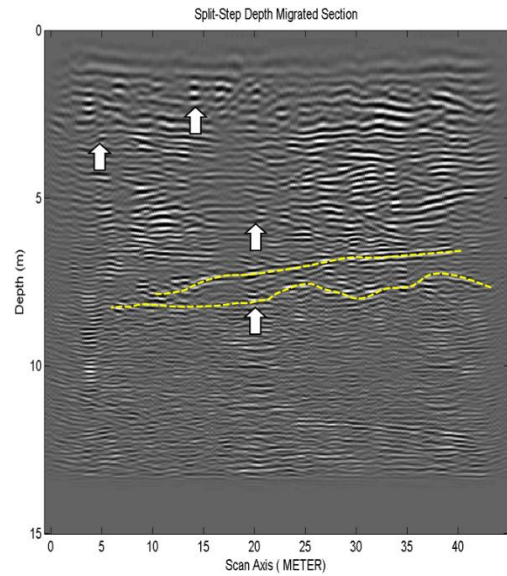


Fig. 8. The GPR migrated section 5

Similarly, we perform all above steps for line 14. The GPR sections before and after migration are shown in fig. 9. We also recognize that all diffraction hyperbolae are collapsed, so the shell deposit boundary becomes easy to see.

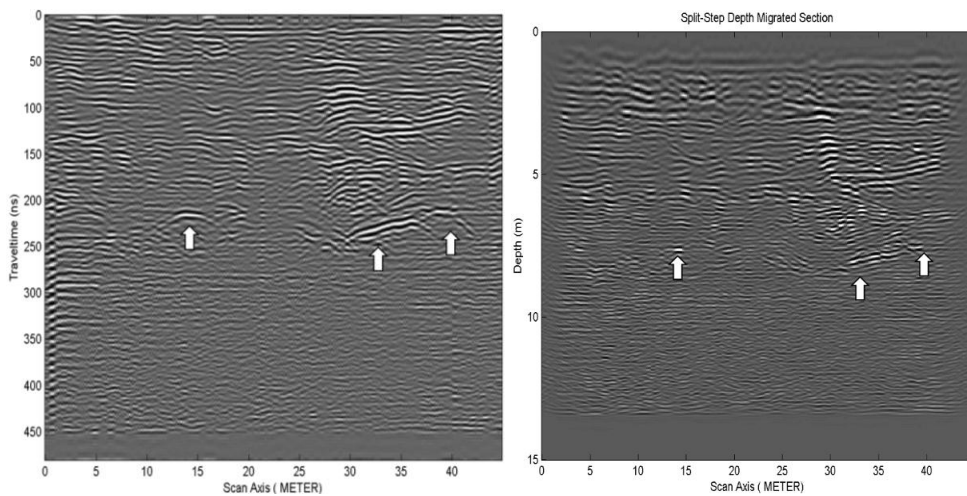


Fig. 9. The GPR section 14 a) before migration; b) after migration

## CONCLUSION

The application of migration methods to interpreting GPR data has advantages and disadvantages as follows:

Energy diagram is a good criterion to optimize the accuracy of determining propagation velocity by migration algorithms.

SSF is depth migration that can be used when the environmental propagation velocity

varies laterally and vertically. The migrated section is clear and it can directly reflect the depth of the apex of objects.

We can calculate exactly the size and the location of objects (example 1) and the depth of shell deposit layer (example 2) in migrated image.

However, the processing steps are complicated. Firstly, we must use time migration to calculate RMS velocity from energy diagram. Secondly, we need to estimate the interval velocity from RMS velocity and build velocity model. Finally, SSF migration method is used to process GPR section.

Therefore, this research should be expanded in the way of using depth migration to calculate energy diagram of each layer. The velocity that has the highest energy can be an interval velocity of this layer. Thus, the processing steps become easier and decrease the error of determining interval velocity.

## REFERENCES

1. Gazdag, J., and Sguazzero, P., 1984. Migration of seismic data. *Proceedings of the IEEE*, **72**(10), 1302-1315.
2. Yilmaz, O., 1987. Seismic Data Analysis, Chapter 4, Society of Exploration Geophysicists, Electronic Edition, ISBN 978-0-931830-46-4, pp. 476-491.
3. Han, B., 1998. A comparison of four depth-migration methods. *68<sup>th</sup> Ann. Internat. Mtg., Soc. Expl. Geophys.* Pp. 1104-1107, doi:10.1190/1.1820080.
4. Stoffa, P. L., Fokkema, J. T., de Luna Freire, R. M., and Kessinger, W. P., 1990. Split-step Fourier migration. *Geophysics*, **55**(4), 410-421.
5. Trung, D. H., Van, N. T., Thuan, N. V., 2016. Migration methods for interpreting GPR data in Vietnam. *Proceedings of workshop on capacity building on geophysical technology in mineral exploration and assessment on land, sea and island, Hanoi.*
6. Van Nguyen, T., Van Le, C. A., Nguyen, V. T., Dang, T. H., Vo, T. M., and Vo, L. N. N., 2017. Energy Analysis in Semiautomatic and Automatic Velocity Estimation for Ground Penetrating Radar Data in Urban Areas: Case Study in Ho Chi Minh City, Vietnam. In *International Conference on Geo-Spatial Technologies and Earth Resources* (pp. 34-51). Springer, Cham.
7. Tzanis, A., 2006. MATGPR: A freeware MATLAB package for the analysis of common-offset GPR data. In *Geophysical Research Abstracts* (Vol. 8, No. 09448).